A SINGLE-CARRIER QUASI-ORTHOGONAL TRANSMISSION SCHEME FOR ASYNCHRONOUS COOPERATIVE RELAY NETWORKS

*M.Hayes, J.A.Chambers, and *M.D.Macleod*

Advanced Signal Processing Group, Dept. of Electronic and Electrical Engineering, Loughborough University, LE11 3TU, UK, and *QinetiQ Ltd, St. Andrews Rd., Malvern, WR14 3PS, UK
Email: {m.hayes, j.a.chambers}@lboro.ac.uk, *mmacleod@signal.qinetiq.com

ABSTRACT

A single-carrier quasi-orthogonal distributed block space-time coding scheme for a wireless collaborative network with one relaying stage composed of four nodes is proposed. This block quasi-orthogonal design can attain full diversity and maximum rate, and is based on simple amplify-and-forward processing at the relay nodes. A cyclic prefix is introduced into the block transmission to overcome channel delay mismatches in the paths through the four relays. In single-carrier operation, these delays are shown to introduce inter-symbol-interference (ISI) in the destination signal. A linear pre-processing scheme is therefore designed to mitigate this ISI through maximizing signal-to-interference-plus-noise ratio (SINR) at the receiver in combination with iterative equalization. To reduce the computational complexity of this scheme the underlying interference matrices are rendered sparse by the pre-processing operation. Simulation studies confirm the improvement in SINR of the proposed approach as compared to one which only uses rectangular pre-windowing.

Index Terms– **Cooperative Systems, Space-Time Coding, Wireless Relay Networks, Asynchronous Communication**

1. INTRODUCTION

Cooperative communication leverages multiple-input multiple-output (MIMO) techniques to increase the available diversity gain in wireless networks with single-antenna relay nodes [1, 2]. Using cooperating relay nodes which overhear the broadcast signal from the source node, it is possible to provide extra observations of the source signal at the destination node. The separated relay nodes mitigate spatial correlation in the MIMO channels, which is known to reduce the BER performance in co-located MIMO systems [3]. However, diversity gain and increased throughput/capacity gains offered in cooperative systems comes at the expense of additional complexity in synchronization between distributed systems both in time and frequency.

In this paper, we consider a parallel relay channel model assuming a single source S communicates with a destination node D utilizing four cooperating relays R_1-R_4, wherein no direct communication between S and D is assumed as illustrated in Fig.1. Separation of the relay nodes makes timing synchronization with the destination node extremely challenging. However, we propose a robust space-time block code (STBC) scheme that is tailored for single-carrier transmission over asynchronous cooperative networks.

In previously developed asynchronous multi-carrier schemes [4, 5] the time-domain modulus of an information symbol can increase by a factor as high as the number of subcarriers used; therefore to avoid introducing nonlinear distortion effects, such as through clipping within the power amplifier, we propose using a single-carrier scheme. However, we demonstrate that single-carrier implementations for non-orthogonal code designs [6] can require additional complexity in decoding due to significant inter-symbol-interference (ISI). To cancel the ISI we propose using a low-complexity iterative receiver design which can be adapted with a variety of scheduling strategies. Since the symbol estimation performance is expected to be proportional to the signal-to-interference-plus-noise ratio (SINR), we investigate the use of a linear pre-processing stage that renders the ISI response sparse and thereby reduces the equalizer complexity.

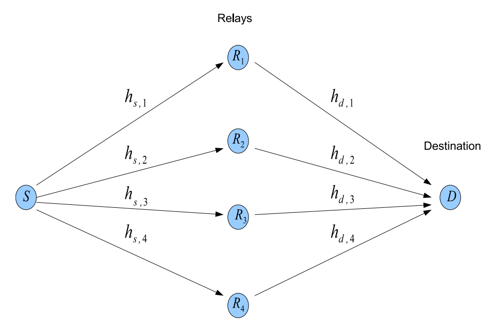

Figure 1: Cooperative two stage relay network architecture

The paper is organized as follows. Section II details the operation of the source and relay nodes. Section III introduces the destination node processing, specifically the initial pre-processing to prepare the data for linear combining. Section IV establishes the use of linear pre-processing to render the ISI response sparse and follows with a description of the equalization stage. Finally, Section V presents simulation results and Section VI concludes with a closing summary.

Notation: In this paper $(\cdot)^*$ is used to denote conjugate, $(\cdot)^T$ transpose and $(\cdot)^H$ conjugate transpose. Bold font denotes matrix and vector descriptions, $D(\mathbf{b})$ denotes a diagonal matrix created from vector $\mathbf{b}$ and $C(\mathbf{b})$ denotes a circulant matrix with the first column $\mathbf{b}$. The matrices F_N, I_N denote an NxN unitary DFT and NxN identity matrix respectively. The element of a matrix $\mathbf{A}$ at the nth row and mth column is denoted by $[\mathbf{A}]_{n,m}$, vector elements are indexed using subscript notation $\mathbf{a}_k$. All indexing variables start at zero. The operator $\Re\{\cdot\}$ returns the real part of a complex argument, $\langle\cdot\rangle_N$ signifies a modulo-N operator and $\odot$ represents the Hadamard product.

2. SYSTEM MODEL

To illustrate, we consider a parallel relay channel from source S to destination node D as shown in Fig.1. The protocol is implemented in two stages; firstly the source broadcasts coded symbols to cooperating relay nodes R_j for $j \in \{1,\ldots,4\}$, the source node then terminates transmission and the relays re-transmit the processed signals to the destination node[1].

To facilitate the use of STBCs all channels in the network are assumed to be quasi-static for the length of the block code. For analysis all channels are assumed to be independent flat Rayleigh fading and are modelled using zero mean circular symmetric complex Gaussian (ZMCSCG) random variables with unity variance.

2.1 First Stage - Source Node Processing

At the source node, complex modulated symbols are grouped into four blocks of length N, represented by the vector $\mathbf{s}^{(i)}$ where $i \in \{1,\ldots,4\}$. Symbol mapping is used to later represent the proposed STBC in the original form [6],

[1]The half-duplex operation of the relay nodes significantly reduces the design complexity at the cost of halving the maximum achievable data-rate.

$$\tilde{\mathbf{s}} = \begin{bmatrix} \mathbf{s}^{(1)} \\ -\mathbf{s}^{(2)*} \\ -\mathbf{s}^{(3)*} \\ \mathbf{s}^{(4)} \end{bmatrix} \tag{1}$$

We assume each block can be subject to a uniformly distributed channel delay with range $[0, \tau_{max})$ and upper bounded by τ_{max}. Without any design consideration inter-block-interference (IBI) is possible between adjacent blocks at the destination. To mitigate IBI we insert a cyclic prefix (CP) of length $N_p \geq \tau_{max}$ at the source increasing the block length to $J = N + N_p$. The modified blocks are denoted as $\sqrt{P_s}\,\mathbf{T}_{cp}\,\mathbf{s}^{(i)}$ with P_s representing the source transmit power, $\mathbf{T}_{cp}$ is illustrated in matrix notation,

$$\mathbf{T}_{cp} = \begin{bmatrix} \mathbf{0}_{N_p\,x\,(N-N_p)} \mid \mathbf{I}_{N_p} \\ \mathbf{I}_N \end{bmatrix}_{J\,\times N} \tag{2}$$

2.2 Relay Node Processing

Each relay R_j receives a noisy copy of the broadcast signal from the source node perturbed by the source-relay flat-fading channel response $h_{s,j}$,

$$\mathbf{r}_j^{(i)} = H_{s,j}(\mathbf{T}_{cp}\mathbf{s}^{(i)}) + \mathbf{v}_j^{(i)} \tag{3}$$

where $H_{s,j} = h_{s,j}\mathbf{I}_N$ is the diagonal channel matrix representing the quasi-static channel between R_j and S. The elements of $\mathbf{v}_j^{(i)}$ are additive white Gaussian noise (AWGN) with zero mean and variance σ^2.

To extract diversity from the relay channel we employ a generalized form of a Jafarkhani [6] quasi-orthogonal STBC based on block encoding,

$$S = \beta \begin{bmatrix} \mathbf{r}_1^{(1)} & -\mathbf{r}_2^{(2)*} & -\mathbf{r}_3^{(3)*} & \mathbf{r}_4^{(4)} \\ \zeta(\mathbf{r}_1^{(2)}) & \zeta(\mathbf{r}_2^{(1)*}) & -\zeta(\mathbf{r}_3^{(4)*}) & -\zeta(\mathbf{r}_4^{(3)}) \\ \zeta(\mathbf{r}_1^{(3)}) & -\zeta(\mathbf{r}_2^{(4)*}) & \zeta(\mathbf{r}_3^{(1)*}) & -\zeta(\mathbf{r}_4^{(2)}) \\ \mathbf{r}_1^{(4)} & \mathbf{r}_2^{(3)*} & \mathbf{r}_3^{(2)*} & \mathbf{r}_4^{(1)} \end{bmatrix}_{4J\,\times 4} \tag{4}$$

where $\zeta(\cdot)$ performs time-reversal on all vector elements as illustrated with an arbitrary vector $\mathbf{a}$,

$$\zeta(\mathbf{a}) = \begin{bmatrix} a(N+N_p-1) \\ \vdots \\ a(0) \end{bmatrix}_{J\,\times 1} \tag{5}$$

Assuming the absence of channel state information (CSI) transmit power allocation for relaying is equally distributed over the relay nodes,

$$\beta = \sqrt{\frac{P_r}{P_s + \sigma^2}} \tag{6}$$

where P_r is the allocated relay power. NB. Relay processing is identical to [5].

3. DESTINATION NODE PROCESSING

3.1 Pre-processing

As a precursor to linear combining pre-processing in the form of CP removal and then re-alignment is required. Without loss of generality we will assume errorless synchronization with R_1 as a basis for CP removal. To re-align the information symbols transmitted on the second and third time-slots a circular shift is implemented,

$$\zeta'(\mathbf{a}[n]) = \mathbf{a}[\langle n - (N_p + 1)\rangle_N] \tag{7}$$

equivalent to an N-point DFT/IDFT applied twice ($\mathbf{P} = \mathbf{F}_N\,\mathbf{F}_N$), i.e.

$$\mathbf{Pa} = [a[0], a[N-1], \ldots, a[1]]^T \tag{8}$$

The equivalent input-output relationship for the collaborative network can now be written as,

$$\begin{bmatrix} \mathbf{y}^{(1)} \\ \mathbf{y}^{(2)*} \\ \mathbf{y}^{(3)*} \\ \mathbf{y}^{(4)} \end{bmatrix} = \begin{bmatrix} H_1 & H_2 & H_3 & H_4 \\ H_2^*\mathbf{P} & -H_1^*\mathbf{P} & H_4^*\mathbf{P} & -H_3^*\mathbf{P} \\ H_3^*\mathbf{P} & H_4^*\mathbf{P} & -H_1^*\mathbf{P} & -H_2^*\mathbf{P} \\ H_4 & -H_3 & -H_2 & H_1 \end{bmatrix} \begin{bmatrix} \mathbf{s}^{(1)} \\ \mathbf{s}^{(2)} \\ \mathbf{s}^{(3)} \\ \mathbf{s}^{(4)} \end{bmatrix} + \begin{bmatrix} \mathbf{w}^{(1)} \\ \mathbf{w}^{(2)*} \\ \mathbf{w}^{(3)*} \\ \mathbf{w}^{(4)} \end{bmatrix} \tag{9}$$

$$\mathbf{y} = \mathbf{Hs} + \mathbf{w} \tag{10}$$

Each equivalent channel matrix H_j shown in (9) is taken as the product of the channel matrices from S-R_j and R_j-D,

$$H_j = \begin{cases} H_{d,j}H_{s,j} & \text{j=1,4} \\ H_{d,j}H_{s,j}^* & \text{j=2,3} \end{cases}$$

where $H_{d,j}$ denotes the response of the channel R_j-D, the product H_j is therefore circulant. It is understood that CP insertion at the transmitter and removal at the receiver converts a linear convolution into a circular convolution [7, Page 202] enabling the channel matrix to be described as a circulant matrix, therefore readily diagonalized by the DFT,

$$\begin{aligned} \mathbf{D}_j &= \mathbf{F}_N H_j \mathbf{F}_N^H \\ &= h_{s,j}\,h_{d,j}\,\mathbf{\Phi}_{\tau_\mathbf{j}} \end{aligned} \tag{11}$$

where $\mathbf{\Phi}_{\tau_\mathbf{j}}$ is a diagonal matrix denoted as,

$$[\mathbf{\Phi}_{\tau_j}]_{k,k} = \begin{cases} e^{-j2\pi k\tau_j/N} & k = 0, 1, \ldots, (N-2)/2 \\ e^{j2\pi(k-N)\tau_j/N} & \text{otherwise} \end{cases} \tag{12}$$

This channel model approximates the linear phase rotations at discretely sampled frequency intervals arising due to the re-transmission delay τ_j associated with signals received via R_j.

3.2 Linear Combining

Efficient linear combining in the frequency-domain is proved possible via exploiting the structure of H_j (11) using the FFT/IFFT algorithm, however we focus on time-domain linear combining for illustrative purposes,

$$\begin{bmatrix} \mathbf{z}^{(1)} \\ \mathbf{z}^{(2)} \\ \mathbf{z}^{(3)} \\ \mathbf{z}^{(4)} \end{bmatrix} = \begin{bmatrix} H_1^H & \mathbf{P}H_2^T & \mathbf{P}H_3^T & H_4^H \\ H_2^H & -\mathbf{P}H_1^T & \mathbf{P}H_4^T & -H_3^H \\ H_3^H & \mathbf{P}H_4^T & -\mathbf{P}H_1^T & -H_2^H \\ H_4^H & -\mathbf{P}H_3^T & -\mathbf{P}H_2^T & H_1^H \end{bmatrix} \begin{bmatrix} \mathbf{y}^{(1)} \\ \mathbf{y}^{(2)*} \\ \mathbf{y}^{(3)*} \\ \mathbf{y}^{(4)} \end{bmatrix} \tag{13}$$

$$\mathbf{z} = \mathbf{H}^H\mathbf{y} \tag{14}$$

Relay reordering (5) and re-alignment at the destination (7) now enable the exploitation of the following properties for any arbitrary circulant matrix $\mathbf{X}$,

$$\mathbf{PXP} = \mathbf{X}^T \text{ and } \mathbf{PX}^*\mathbf{P} = \mathbf{X}^H \tag{15}$$

as shown in (13). If we consider the overall input-output relationship it is relatively straightforward to combine (10)-(14) into a simple model,

$$\mathbf{z} = \mathbf{As} + \mathbf{H}^H\mathbf{w} \tag{16}$$

which decouples the information blocks $\{\mathbf{s}^{(1)}, \mathbf{s}^{(4)}\}$ and $\{\mathbf{s}^{(2)}, \mathbf{s}^{(3)}\}$ simplifying the equalization stage as illustrated by expanding the matrix $\mathbf{A}$,

$$\mathbf{A} = \begin{bmatrix} \mathbf{\Gamma} & \mathbf{0} & \mathbf{0} & \mathbf{\Lambda} \\ \mathbf{0} & \mathbf{\Gamma} & -\mathbf{\Lambda}^T & \mathbf{0} \\ \mathbf{0} & -\mathbf{\Lambda}^T & \mathbf{\Gamma} & \mathbf{0} \\ \mathbf{\Lambda} & \mathbf{0} & \mathbf{0} & \mathbf{\Gamma} \end{bmatrix} \tag{17}$$

are retained as contributions from Γ and Λ. The parameter D controls the number of additional observations used in the estimation process at the expense of increased computation of the covariance matrix inversion performed in linear MMSE estimation. In Section V the relationship between τ_{max} and SINR are presented for variations of the parameter D.

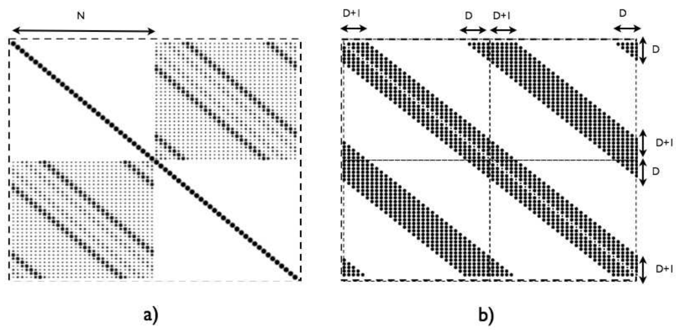

Figure 2: a) discrete representation of the coupling matrix $\breve{\mathbf{A}}$ b) binary masking operator M with width parameter D

In (17) it is shown that $\mathbf{A}$ is composed of diagonal matrix $\mathbf{\Gamma}$ and an 'interference' matrix $\mathbf{\Lambda}$,

$$\mathbf{\Gamma} = \mathbf{F}^H \left(\sum_{j=1}^{4} |\mathbf{D}_j|^2 \right) \mathbf{F} \tag{18}$$

$$\mathbf{\Lambda} = 2\mathbf{F}^H \left(\Re \{ \mathbf{D}_4^* \mathbf{D}_1 - \mathbf{D}_3 \mathbf{D}_2^* \} \right) \mathbf{F} \tag{19}$$

In the next section we exploit the structure (16)-(19) to perform low-complexity equalization.

4. ITERATIVE SYMBOL ESTIMATION

Taking the preprocessed observation $\mathbf{z}$ (16) the destination node can now estimate the transmitted symbols $\mathbf{s}$ in the presence of ISI. In the problem formulation we assume a non-zero matrix $\mathbf{\Lambda}$ (19), therefore requiring an equalization stage to infer the coded symbols from the observation. Exploiting the structure of (17) equalization can be performed in parallel on two decoupled subsystems $\{\mathbf{z}^{(1)}, \mathbf{z}^{(4)}\}$ and $\{\mathbf{z}^{(2)}, \mathbf{z}^{(3)}\}$. We illustrate this using only one of the subsystems $\{\mathbf{z}^{(1)}, \mathbf{z}^{(4)}\}$ as an example,

$$\begin{bmatrix} \mathbf{z}^{(1)} \\ \mathbf{z}^{(4)} \end{bmatrix} = \begin{bmatrix} \mathbf{\Gamma} & \mathbf{\Lambda} \\ \mathbf{\Lambda} & \mathbf{\Gamma} \end{bmatrix} \begin{bmatrix} \mathbf{s}^{(1)} \\ \mathbf{s}^{(4)} \end{bmatrix} + \begin{bmatrix} H_1^H & \mathbf{P}H_2^T & \mathbf{P}H_3^T & H_4^H \\ H_4^H & -\mathbf{P}H_3^T & -\mathbf{P}H_2^T & H_1^H \end{bmatrix} \begin{bmatrix} \mathbf{w}^{(1)} \\ \mathbf{w}^{(2)*} \\ \mathbf{w}^{(3)*} \\ \mathbf{w}^{(4)} \end{bmatrix} \tag{20}$$

$$\breve{\mathbf{z}} = \breve{\mathbf{A}}\breve{s} + \breve{\mathbf{H}}\mathbf{w} \tag{21}$$

An illustration of the location of non-zero elements of $\breve{\mathbf{A}}$ is shown in Fig.2 a).

4.1 Rectangular Windowing

The reduced order subsystems (21) are still computationally expensive $O(N^3)$ for performing the necessary matrix inversion involved in minimum mean square error (MMSE) estimation. We propose reducing the complexity to $O(D^3)$, where $D << N$, by retaining only the significant elements of $\breve{\mathbf{A}}$. This is performed using a binary masking operation M, i.e. $M \odot \breve{\mathbf{A}}$, to target the ISI-response to a given rectangular window of width $2D+1$. The shaded regions in Fig.2 b) show the retained elements of $\breve{\mathbf{A}}$ after masking. Fig.2 b) specifically illustrates that the 2D + 1 central diagonals, a D x D lower triangular matrix in the bottom left corner and a D x D upper triangular matrix are retained as contributions from Γ and Λ.

4.2 Open Loop Linear Preprocessing

To maximize the SINR we propose a linear preprocessing stage prior to MMSE symbol estimation that renders the ISI response sparse. The structure of the interference matrix (19) facilities preprocessing that confines the signal energy into the residual coefficients retained after the masking is performed. The parameter D then effectively controls the target ISI-response length and the computational complexity of the MMSE decoder. We consider only a window design for subsystem (21), however it is straightforward to generalize for the other subsystem not specified.

4.2.1 Frequency-Domain ISI shortening

Single-carrier systems can achieve ISI-shortening via convolutive linear filtering, however we propose leveraging the FFT used in frequency domain combining to perform fast convolution in the frequency domain therefore increasing efficiency when N is large. For example in matrix notation fast convolution for the system denoted by (21) can be written as,

$$\begin{aligned} \breve{\mathbf{x}} &= T(\nu)\breve{\mathbf{z}} && (22) \\ &= T(\nu)\breve{\mathbf{A}}\breve{s} + T(\nu)\breve{\mathbf{H}}\mathbf{w} && (23) \end{aligned}$$

assuming,

$$T(\nu) = \begin{bmatrix} C(\nu) & \mathbf{0}_N \\ \mathbf{0}_N & C(\nu) \end{bmatrix} \tag{24}$$

where ν denotes the time-domain impulse response of the shortening filters corresponding to the first/last N rows of $\breve{\mathbf{A}}$. The frequency-domain equivalent linear processing may be expressed as,

$$\mathbf{b} := \breve{\mathbf{F}}\nu \tag{25}$$

where $\beta = [\mathbf{b}^T \mathbf{b}^T]^T$ is the frequency-domain representation of the shortening filter impulse response and

$$\breve{\mathbf{F}} = \begin{bmatrix} \mathbf{F}_N & \mathbf{0}_N \\ \mathbf{0}_N & \mathbf{F}_N \end{bmatrix} \tag{26}$$

It is then simple to show that ISI mitigation can be performed in the frequency-domain,

$$\breve{\mathbf{x}} = \breve{\mathbf{F}}^H D(\beta) \breve{\mathbf{F}} \breve{\mathbf{z}} \tag{27}$$

which demonstrates that the linear preprocessing can be performed in the frequency domain after linear combining.

4.2.2 Maximizing SINR

Utilizing the symmetry in the symbol coupling matrices shown in (20) we can formulate the SINR optimization based on the following reduced order system,

$$\begin{aligned} \breve{\mathbf{x}}^{(i)} &= C(\nu)\mathbf{z}^{(i)} && (28) \\ &= C(\nu)\breve{\mathbf{A}}^{(i)}\breve{s} + C(\nu)\breve{\mathbf{H}}^{(i)}\mathbf{w} && (29) \end{aligned}$$

which follows from (20)-(21) using the definitions below,

$$\breve{\mathbf{A}}^{(1)} := \begin{bmatrix} \mathbf{\Gamma} & \mathbf{\Lambda} \end{bmatrix} \;\; \breve{\mathbf{A}}^{(4)} := \begin{bmatrix} \mathbf{\Lambda} & \mathbf{\Gamma} \end{bmatrix}$$

$$\breve{\mathbf{H}}^{(1)} := \begin{bmatrix} H_1^H & \mathbf{P}H_2^T & \mathbf{P}H_3^T & H_4^H \end{bmatrix}$$
$$\breve{\mathbf{H}}^{(4)} := \begin{bmatrix} H_4^H & -\mathbf{P}H_3^T & -\mathbf{P}H_2^T & H_1^H \end{bmatrix}$$

To define the optimization problem we sub-divide the symbol coupling matrix $\breve{\mathbf{A}}^{(i)}$ into a 'desired' signal component which is retained after masking and an interference plus noise component. Assuming $E\{\breve{s}\breve{s}^H\} = \mathbf{I}_{2N}$ it can be shown that the Frobenius norm representing the desired signal ε_s and total signal energy ε_t can be express as,

$$\begin{aligned} \varepsilon_s &= \|M \odot (C(\nu)\breve{\mathbf{A}})\|_F^2 && (30) \\ &= \mathbf{b}^H \left(\mathbf{S} \odot (\mathbf{F}(\Gamma\,\Gamma^H + \Lambda\,\Lambda^H)\mathbf{F}^H)\right)\mathbf{b} && (31) \end{aligned}$$

$$\begin{aligned} \varepsilon_t &= \|(C(\nu)\breve{\mathbf{A}})\|_F^2 + \sigma_w^2\|C(\nu)\breve{\mathbf{H}}\|_F^2 && (32) \\ &= \mathbf{b}^H diag\left(\mathbf{F}(\Gamma\,\Gamma^H + \Lambda\,\Lambda^H + \sigma_w^2.\Gamma)\mathbf{F}^H\right)\mathbf{b} && (33) \end{aligned}$$

where,

$$[\mathbf{S}]_{n,m} := \frac{\sin\left(\frac{\pi}{N}(2D+1)(n-m)\right)}{N\sin\left(\frac{\pi}{N}(n-m)\right)} \quad (34)$$

The optimization problem can then be specified in generalized eigenvalue form,

$$\mathbf{b}^* := \arg\max_{\mathbf{b}} \frac{\varepsilon_s}{\varepsilon_t - \varepsilon_s} \quad (35)$$

where we denote the optimal solution using the notation $(\cdot)^*$.

4.3 Iterative MMSE equalizer

In the following formulation we only consider the structuring of data for estimating $\mathbf{s}^{(1)}$ and do not include elements outside the rectangular window; it is straightforward to generalize the estimation process for other blocks from this description. To formulate our low-complexity equalizer design, only elements in the observation $\breve{\mathbf{z}}$ (21) which are contributions from $\breve{\mathbf{s}}$ after windowing are retained, rendering the new observation vector,

$$\breve{\mathbf{z}}_k := \left[\breve{z}_{<k-D>_N}, \ldots, \breve{z}_{<k+D>_N}, \breve{z}_{<k-D>_N+N}, \ldots, \breve{z}_{<k+D>_N+N}\right]^T \quad (36)$$

For the remainder of this discussion unless otherwise stated all indexing in this section is taken as Modulo-N. To incorporate linear preprocessing we use the definitions $\breve{\mathbf{\Lambda}} := C(\nu)\mathbf{\Lambda}$ and $\breve{\mathbf{\Gamma}} := C(\nu)\mathbf{\Gamma}$. Assuming the channel shortening restricts the ISI to lie inside the masking operator shown in Fig.2 b) the subsystem vectors and matrices can be re-written as,

$$\breve{\mathbf{\Lambda}}_k := \begin{bmatrix} [\breve{\mathbf{\Lambda}}]_{k-D,k-2D} & \cdots & [\breve{\mathbf{\Lambda}}]_{k-D,k} & & \\ & \ddots & \vdots & \ddots & \\ & & [\breve{\mathbf{\Lambda}}]_{k+D,k} & \cdots & [\breve{\mathbf{\Lambda}}]_{k+D,k+2D} \end{bmatrix} \quad (37)$$

$$\breve{\mathbf{\Gamma}}_k := \begin{bmatrix} [\breve{\mathbf{\Gamma}}]_{k-D,k-2D} & \cdots & [\breve{\mathbf{\Gamma}}]_{k-D,k} & & \\ & \ddots & \vdots & \ddots & \\ & & [\breve{\mathbf{\Gamma}}]_{k+D,k} & \cdots & [\breve{\mathbf{\Gamma}}]_{k+D,k+2D} \end{bmatrix} \quad (38)$$

$$\mathbf{C}_k := \begin{bmatrix} [\nu]_{k-D} & [\nu]_{k-D-1} & \cdots & [\nu]_{k-D-N+1} \\ [\nu]_{k-D+1} & [\nu]_{k-D} & \cdots & [\nu]_{k-D-N+2} \\ \ddots & \ddots & \ddots & \ddots \\ [\nu]_{k+D} & [\nu]_{k+D-1} & \cdots & [\nu]_{k+D-N+1} \end{bmatrix} \quad (39)$$

$$\breve{\mathbf{C}}_k := \begin{bmatrix} \mathbf{C}_k & \mathbf{0} \\ \mathbf{0} & \mathbf{C}_k \end{bmatrix} \quad (40)$$

$$\breve{\mathbf{A}}_k := \begin{bmatrix} \breve{\mathbf{\Gamma}}_k & \breve{\mathbf{\Lambda}}_k \\ \breve{\mathbf{\Lambda}}_k & \breve{\mathbf{\Gamma}}_k \end{bmatrix} \quad (41)$$

$$\breve{\mathbf{s}}_k := \left[\breve{s}_{<k-D>_N}, \ldots, \breve{s}_{<k+D>_N}, \breve{s}_{<k-D>_N+N}, \ldots, \breve{s}_{<k+D>_N+N}\right]^T \quad (42)$$

defining the new equalization problems as,

$$\breve{\mathbf{z}}_k = \breve{\mathbf{A}}_k\breve{\mathbf{s}}_k + \breve{\mathbf{w}}_k \quad (43)$$

where $\breve{\mathbf{w}}_k$ represents the processed AWGN induced at the destination and relay nodes. The noise covariance matrix is defined in the next section, however because of constraints on space the derivation of $\breve{\mathbf{w}}_k$ is left to the interested reader.

4.3.1 Linear MMSE estimator

Although each symbol defined by s_k belongs to a finite alphabet Ω, we assume temporarily that the vector $\breve{\mathbf{s}}_k$ has the a-priori Gaussian distribution $\breve{\mathbf{s}}_k \sim N_C(\mathbf{m}_a, \Sigma_a)$, assuming,

$$\begin{aligned} \mathbf{m}_a &= E\{\breve{\mathbf{s}}_k\} && (44) \\ \Sigma_a &= E\{(\breve{\mathbf{s}}_k - \mathbf{m}_a)(\breve{\mathbf{s}}_k - \mathbf{m}_a)^H\} && (45) \end{aligned}$$

This justifies the use of a linear MMSE estimator where $\breve{\mathbf{z}}_k$ and $\breve{\mathbf{s}}_k$ can be assumed jointly Gaussian giving the linear MMSE estimate,

$$\hat{\mathbf{s}} = \mathbf{m}_a + \Sigma_{SZ}\Sigma_{ZZ}^{-1}(\breve{\mathbf{z}}_k - \mathbf{m}_{\breve{\mathbf{z}}_k}) \quad (46)$$

The symbols Σ_{ZZ} and Σ_{SZ} define auto and cross-covariance matrices associated with the observation and transmitted symbol random variables. In addition if we assume prior information

$$\begin{aligned} E\{\breve{\mathbf{w}}_k\} &= \mathbf{0} && (47) \\ E\{\breve{\mathbf{w}}_k\breve{\mathbf{w}}_k^H\} &= \Sigma_{WW} && (48) \\ E\{\breve{\mathbf{s}}_k\breve{\mathbf{w}}_k^H\} &= \mathbf{0} && (49) \\ E\{\breve{\mathbf{s}}_k\breve{\mathbf{s}}_k^H\} &= \Sigma_a && (50) \end{aligned}$$

then it is possible to show,

$$\begin{aligned} \Sigma_{ZS} &= \Sigma_a\breve{\mathbf{A}}_k^H && (51) \\ \Sigma_{ZZ} &= \breve{\mathbf{A}}_k\Sigma_a\breve{\mathbf{A}}_k^H + \Sigma_{WW} && (52) \\ \mathbf{m}_{\breve{\mathbf{z}}_k} &= \breve{\mathbf{A}}_k\mathbf{m}_a && (53) \end{aligned}$$

where the noise covariance[2] matrix is given by,

$$\Sigma_{WW} = \sigma_w^2\mathbf{C}_k\breve{\mathbf{A}}\mathbf{C}_k^H \quad (54)$$

assuming,

$$\sigma_w^2 = \sigma^2\left(\beta^2\sum_{j=1}^{4}|h_{d,j}|^2 + 1\right) \quad (55)$$

[2]After combining the noise can no longer be considered uncorrelated.

4.3.2 Calculating the priors

In the first iteration of the equalization stage we initialize all priors using (44), (45) and (51)-(53). Under a conditional Gaussian assumption the a-posteriori probability for $\hat{\mathbf{s}}_k$ can then be determined,

$$P\left(s_k|\breve{\mathbf{z}}_k, \breve{\mathbf{A}}_k\right) \propto \exp\left(-\frac{1}{\sigma^2_{p,\,k}}|s_k - \hat{s}_{p,\,k}|^2\right) \tag{56}$$

assuming the first and second order statistics are

$$\hat{s}_{p,\,k} = \mathbf{e}^T\left(\mathbf{m}_a + \Sigma_{ZS}\Sigma_{ZZ}^{-1}(\breve{\mathbf{z}}_k - \mathbf{m}_{\breve{\mathbf{z}}_k})\right) \tag{57}$$

$$\sigma^2_{p,\,k} = \mathbf{e}^T\left(\Sigma_a - \Sigma_{ZS}\Sigma_{ZZ}^{-1}\breve{\mathbf{A}}_k)\Sigma_a\right)\mathbf{e} \tag{58}$$

where $\mathbf{e} = [1_1\ 0_2 \ldots 0_{2D+2}]^T$ is used as a selection vector. After the first iteration extrinsic information can be calculated,

$$m_{e,\,k} = \sum_{s_k\in\Omega} s_k\ \cdot P\left(s_k|\breve{\mathbf{z}}_k, \breve{\mathbf{A}}_k\right) \tag{59}$$

$$\sigma^2_{e,\,k} = \sum_{s_k\in\Omega} |s_k - m_{e,\,k}|^2\ \cdot P\left(s_k|\breve{\mathbf{z}}_k, \breve{\mathbf{A}}_k\right) \tag{60}$$

To accurately obtain the new priors and decouple from the estimates derived in a previous iteration we use only extrinsic information from other interfering symbols, i.e. $\hat{s}_i$ for $i \neq k$, therefore attempting to minimize error propagation. If we make the assumptions $\frac{1}{|\Omega|}\sum_{s\in\Omega} s = 0$ and $\frac{1}{|\Omega|}\sum_{s\in\Omega}|s|^2 = 1$ then the new extrinsic information can be constructed for the kth symbol estimate,

$$\mathbf{m}_{\bar{k}} = [0_k\ \ m_{e,<k-D>_N+N}\ldots m_{e,<k+D>_N+N}]^T \tag{61}$$

$$\Sigma_{\bar{k}} = D\left(1_k\ \ \sigma^2_{e,<k-D>_N+N}\ldots\sigma^2_{e,<k+D>_N+N}\right) \tag{62}$$

Based on the updated extrinsic information the probability of the new priors can now be calculated,

$$P\left(s_k|\breve{\mathbf{z}}_k, \breve{\mathbf{A}}_k\right) \propto \exp\left(-\frac{1}{\sigma^2_{e,\,k}}|s_k - \hat{s}_{e,\,k}|^2\right) \tag{63}$$

where the Gaussian pdf is fully defined by,

$$\hat{s}_{e\,,\,k} = \mathbf{p}_k^H\left(\breve{\mathbf{z}}_k - \breve{\mathbf{A}}_k\mathbf{m}_{\bar{k}}\right) \tag{64}$$

$$\sigma^2_{e,\,k} = 1 - \mathbf{p}_k^H\mathbf{a}_k \tag{65}$$

using the following substitutions for simplicity,

$$\mathbf{p}_k = \left(\breve{\mathbf{A}}_k\Sigma_{\bar{k}}\breve{\mathbf{A}}_k^H + \Sigma_{WW}\right)^{-1}\mathbf{a}_k \tag{66}$$

$$\mathbf{a}_k = \breve{\mathbf{A}}_k\mathbf{e} \tag{67}$$

The new probability mass function (63) can then be used to populate extrinsic information (61)-(62) for the next iteration.

5. SIMULATION RESULTS

In this section we present Monte-Carlo based simulation results for the proposed scheme. Simulations are based on N = 32 symbols per frame, i.i.d. ZMCSCG channel realization and noise with unity and SNR^{-1} variance respectively. QPSK modulation is assumed as the symbol alphabet. We assume perfect channel state information at the destination (decoding) node.

Fig.3 shows the channel-averaged SINR performance of various window sizes with and without linear pre-processing (10,000 channel realizations). We consider an SNR of 25dB at the destination node before linear combining is performed. Fig.3 clearly demonstrates that linear combining and our definition of the signal contribution (30) for equalization results in an SINR above 25dB. However, taking the synchronous case as a base point for comparison, i.e. $\tau_{max} = 0$, it is clear that using optimal linear pre-processing (max-SINR) significantly improves the SINR over just rectangular windowing (rect) for high τ_{max} and reduces the window size requirements D. Fig.3 also suggest a positive correlation between τ_{max} and generation of ISI outside of the banded rectangular window, therefore supporting the increase in window size when the upper bounded delay τ_{max} is relaxed which shows a performance increase at the cost of higher receiver complexity.

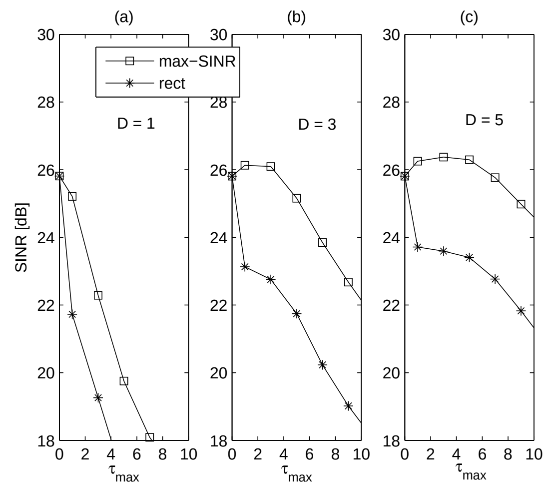

Figure 3: SINR versus τ_{max} for N = 32, SNR = 25 dB, Rayleigh fading, and various D.

6. CONCLUSION

This paper has introduced a novel quasi-orthogonal space-time transmission scheme for use in asynchronous wireless relay networks. Single-carrier quasi-orthogonal transmission however comes at the price of increased ISI between transmitted symbols compared to multi-carrier counterparts, leading to the requirement for equalization. In this paper we demonstrated a low-complexity soft ISI-cancelling iterative equalizer design which leverages linear pre-processing to render the ISI-response sparse and maximize SINR for a given target response length D, therefore resulting in reducing complexity of the order $O(N^3)$ to $O(D^3)$ where $D << N$.

REFERENCES

[1] A.Sendonaris, E.Erkip and B.Aazhang, "User Cooperation Diversity - Part I: System Description" *IEEE Trans. Comms*, Vol. 51(11), pp. 1927-1937, Nov 2003.

[2] J.N.Laneman, *Cooperative Diversity in Wireless Networks: Algorithms and Architectures*. PhD Thesis, MIT, Sept 2002.

[3] A.Paulraj, R.Nabar and D.Gore, *Introduction to Space-Time Wireless Communications*. Cambridge University Press, 2003.

[4] Z.Li and X.Xia, "A Simple Alamouti SpaceTime Transmission Scheme for Asynchronous Cooperative Systems," *IEEE Signal Processing Letters*, vol. 14, pp. 804-4, Nov 2007.

[5] M.Hayes, J.A.Chambers and M.D.Macleod, "A Simple Quasi-Orthogonal Space-Time Scheme for use in Asynchronous Virtual Antenna Array Enabled Cooperative Networks ," in *Proc. EPSRC 2008*, Lausanne, Aug 25-29 2008.

[6] H.Jafarkhani, "A Quasi-Orthogonal Space-Time Block Code," *IEEE Trans. Inform. Theory*, vol. 45, pp. 1-4, Jan 2001.

[7] G.H.Golub and C.F.van Loan, *Matrix Computations*. 3rd ed., Johns Hopkins University Press, Baltimore, 1996.